



OPEN First observation of genus *Komarekiella* in Iranian saline soils

Marzieh Ghadirli¹, Setareh Haghighat^{1✉}, Bahareh Nowruzi^{2✉}, Rambod Norouzi³ & Lenka Hutarova⁴

Cyanobacteria are key elements of saline soils, particularly in the formation of vast surface crusts in arid regions and mine spoil wastes. These microorganisms are also abundant in areas that subjected to periodic wetting and submergence. In fact, sheaths or mucilage and its component polysaccharides have important effects in improving soil structure in saline environments. In our current research, we studied a nitrogen-fixing cyanobacterium obtained from saline soils in Golestan Province, Iran. We used a polyphasic analysis, combining both morphological and molecular techniques. Phylogenetic analysis was performed via the complete sequence of the 16S rRNA gene, along with 16S-23S internal transcribed spacer (ITS) secondary structures. Further determinants were investigated using the sequences of the *nifD*, *psbA*, and *rbcl* genes. The isolates were assigned to the genus *Komarekiella* on the basis of 16S rRNA phylogenetic analysis with 98.80 to 100% similarity to other species of this genus. The 16S-23S ITS fold structures of the D1-D1', Box-B, and V2 helical regions distinguished the isolates from known *Komarekiella* species. Furthermore, ITS *p*-distances between the studied strain and related taxa revealed that the *Komarekiella* sp. isolate 1400 shared an ITS sequence similarity of 98.20 to 98.47% with the *Komarekiella atlantica* species. These results increase our knowledge of the biodiversity and characterisation of the heterocystous genus *Komarekiella* in the saline soils of Iran, isolated for the first time from this type of environment.

Keywords Cyanobacteria, Biofertilization, Nostocales, 16S rRNA gene phylogeny, Polyphasic approach, Saline soils

Saline soils around the world have been devastated by the prolonged use of chemical fertilisers and frequent irrigation. This has led to widespread erosion, nutrient depletion, and increased salinity levels¹. Cyanobacteria are photosynthetic prokaryotes with diverse morphologies, that thrive in environments ranging from terrestrial ecosystems to aquatic systems. These microbes have evolved unique traits, such as the ability to form symbiotic relationships with plants and other species. The relationship between cyanobacteria and plants is particularly important, as cyanobacteria play a crucial role in plant development, stress tolerance and disease prevention. Beyond these primary functions, cyanobacteria contribute to several ecological processes, including nitrogen fixation, phosphate solubilisation, phytohormone biosynthesis, and indirect hostility to pathogens through the production of siderophores¹.

The classification of the phylum Cyanobacteria presents challenges resulting in numerous revisions over time². In addition, some morphological characteristics can vary significantly under different environmental conditions, make species identification difficult when based on physical characteristics alone.

The cyanobacterial genus *Komarekiella* belongs to the family Nostocaceae and the order Nostocales. It is particularly important for saline soils without additional nitrogen inputs due to its ability to fix nitrogen, thereby improving soil quality and human income³. With members of this genus morphologically identical to those of *Nostoc sensu strictu*, new nostocacean genera have been proposed: *Mojavia*⁴, *Desmonostoc*², *Halotia*⁵, *Aliinostoc*⁶, *Komarekiella*³, *Desikacharya*⁷, and *Minunostoc*⁸. *Komarekiella* filaments differ from typical *Nostoc* filaments in that they do not form clearly visible mucilaginous colonies as in the previously listed species. The genus *Komarekiella* is distinguished from other cyanobacterial taxa such as *Desmonostoc*, *Halotia*, *Mojavia*, and tiny *Nostoc* by a distinct type of akinete sprouting. At the molecular level, *Komarekiella* is most similar to *Goeter apudmare*. However, *Goeter apudmare* has some notable differences such as heteromorphic uniform

¹Department of Microbiology, Faculty of Advanced Sciences and Technology, Tehran Medical Sciences Branch, Islamic Azad University, Tehran, Iran. ²Department of Biotechnology, Faculty of Converging Sciences and Technologies, Science and Research Branch, Islamic Azad University, Tehran, Iran. ³Department of Molecular Biosciences, Autonomous University of Madrid, Madrid, Spain. ⁴Institute of Biology and Biotechnology, Faculty of Natural Sciences, University of Ss. Cyril and Methodius in Trnava, Trnava, Slovakia. ✉email: setareh_haghighat@yahoo.com; bahareh.nowruzi@srbiau.ac.ir

trichomes with obvious tapering and basal heterocyst, akinete formation occurs in series, and *Chlorogloeopsis*-like spherical colonies are completely absent³. Phylogenetic analysis revealed that *Komarekiella* form a distinct group separate from closely related groups such as *Nostoc*, *Halotia*, and *Mojavia*^{5,6,9,10}. *Komarekiella* are typically found in nonhostile environments³.

Nowadays, the genus *Komarekiella* is represented by five different species. The type species of the genus is *Komarekiella atlantica*, which colonises concrete walls, wood, bark and other terrestrial habitats³. *Komarekiella globulosa*¹¹ and *Komarekiella gloeocapsoides*¹¹, which are often isolated as a cyanobionts from lichens. *Komarekiella chia*¹², isolated from epilithic maths in the calcareous substrate in caves. *Komarekiella delphini-convector*¹³ the epizoic species isolated from dead bottlenose dolphins. Nine *Komarekiella atlantica* isolates are known, to the date: *Komarekiella atlantica* CCIBT 3483 (KX638487), *Komarekiella atlantica* CCIBT 3481 (KX638484), *Komarekiella atlantica* CCIBT 3487 (KX638488), *Komarekiella atlantica* CCIBT 3552 (KX638485), *Komarekiella atlantica* CCIBT 3486 (KX638489), *Komarekiella atlantica* HA4396-MV6 (KX646832), *Komarekiella atlantica* HA4396-MV6 (KX646831), *Komarekiella atlantica* MTQ17-MM2 (MW344113) and *Komarekiella atlantica* MTQ8-MM1A (MW344112)³.

In addition to the 16S rRNA gene phylogeny, the secondary structures of the 16S–23S rRNA ITS region are frequently employed to improve the precision of cyanobacterial species classification^{14–17}. Despite the potential for substantially divergent results, diagnostic genes such as *nifD*^{18,19}, *psbA*²⁰ and *rbcL* genes¹⁸ are useful as additional or independent determinants for inferring phylogenetic relationships within cyanobacteria²⁰.

Studies concerning the diversity of heterocyst-forming cyanobacteria from saline soils in Iran are scarce, which may make their use as biofertilisers difficult. A *Komarekiella* isolate obtained from Iranian saline soils was molecularly and morphologically characterized, so that our findings can help to increased knowledge of the biodiversity of nostocacean cyanobacteria biodiversity in saline soils, with the expectation that future studies can develop inoculants to improve saline soil structure.

Materials and methods
On-site investigation

In October 2020, cyanobacterial biomass was collected from a saline soil area at coordinates of 36°51'25''N and 54°26'55''E in Gorgan city, Golestan province, Iran. Soil samples were obtained from the upper 5 cm layer and transported to the laboratory for cyanobacterial extraction and analysis. The information about the soil characteristics is listened in (Table 1).

Isolation and morphological assessment of cyanobacteria

Small fragments of the cyanobacterial mat were cultured in liquid BG-11²¹. The biomass was periodically examined under a microscope to isolate a single colony. The isolated colony was first labelled1355 and stored in an Erlenmeyer flask (250 mL) containing liquid BG-11. It was incubated at 28±2 °C exposed to light at approximately 50–55 μmol photons m⁻² s⁻¹ and maintained on a 14 h L/10 h D cycle.

Morphological analysis was performed using an Olympus CX31RTS5 stereoscope and an Olympus BX43 microscope (Olympus, Tokyo, Japan), both of which were equipped with digital cameras.

Morphology changes were observed regularly during the log phase of growth, checked monthly and photographed to detect any morphological differences. Cell measurements were taken using DP-SOFT software, with 50 to 200 measurements per parameter used to assess the variability of the characteristics. The isolate was identified following the guidelines of²², with additional insights from recent studies on the description of new *Komarekiella* species³. In the morphological description we focused on morphological characters such as: thallus, filaments, false branching, filament and cell sizes, leaves, color of trichomes and thallus, presence of mucilage, presence and type of akinete and heterocyst.

The obtained fresh cultures and exsiccates will be deposited in the cyanobacteria culture collection (CCC) and the ALBORZ Herbarium at the Science and Research Branch, Islamic Azad University (Tehran).

Parameters	Mean values
pH	7.9
soil salinity (millimhos/cm)	17.2–18.5
Temperature (°C)	325.5
Dissolved oxygen (mg/L)	3–9.02
Depth (cm)	0.5
Free carbon dioxide (mg/L)	25.1
Alkalinity (mg/L)	71/1
Calcium (mg/L)	21.9
Magnesium (mg/L)	4.9
Total phosphate (μg/L)	199.3
Nitrate nitrogen (μg/L)	319.06

Table 1. Limnological parameters of the sample site.

PCR amplification of 16S rRNA and ITS regions

A 16-day bacterial culture was used to purify genomic DNA with the HiPurA™ Bacterial Genomic DNA Purification Kit (HiMedia). Extended incubation times of 60 and 20 min were used for lysis solutions AL and C1, respectively. The 16S rRNA gene was amplified using forward and reverse primers in a PCR reaction with 1×DyNAzyme PCR buffer, 0.5 µM of each primer, 0.5 U Taq polymerase, 1 µL of DNA (140 ng), and water (Thermocycling programs are illustrated in Table S1). The ITS region was amplified with ITSF/ITSR primers and 18 internal primers for the 16S rRNA gene (Table S2). Cloning was done using the TOPO TA system, with transformation into TOPO10 *E. coli* cells and selection using X-gal and ampicillin. Screening for *nifD*, *psbA*, and *rbcL* was performed using specific primers, 1.5 mM MgCl₂, and Taq polymerase. The PCR products were checked by gel electrophoresis, visualized under UV light, and quantified before sequencing with the BigDye® Terminator Kit. The target sequences were sequenced in both directions, with data collected from a minimum of three independent sequencing reactions (Phred score ≥ 20). The sequenced segments were combined into contigs utilizing BioEdit Sequence Alignment Editor version 7²³. Sequences were aligned using BioEdit and compared to those in the NCBI databases via BLASTn and BLASTX, with coding regions annotated using the NCBI ORF Finder and ExPASy proteomics servers.

Nucleotide sequence accession numbers

Sequence data for 16S rRNA, *nifD*, *psbA* and *rbcL* were recorded in the DNA Data Bank of Japan (DDBJ) under the accession numbers OR669676, OP851553, OP851552 and OP846527, respectively (Table S3).

Phylogenetic analysis

The gene sequences obtained in this study were aligned with similar sequences (≥ 94% identity) from GenBank using MAFFT version 7. IQ-TREE (multicore v1.5.5) was then used to infer phylogenetic trees for the 16S rRNA, *nifD*, *psbA*, and *rbcL* genes, which had base pair sequences of 396, 88, 63, and 62 nucleotides, respectively²⁴. The best-fit models were selected according to the Bayesian Information Criterion (BIC) following a model test in IQ-TREE (Table S3). Tree reliability was assessed using both standard bootstrap (100 replicates) and ultrafast bootstrap (10,000 replicates) to evaluate branch support. Phylogenetic trees were visualized with Fig Tree version 1.2.2²⁵. *Gloeobacter violaceus* was adopted as an outgroup in all phylogenetic.

16S-23S rRNA ITS region secondary structure analysis

The sequence covering the D1-D1' helix, D2, D3, BOX B, BOX A and D4 regions of the 16S-23S ITS in the strain under study was characterized based on²⁶. The ITS secondary structures of the studied strain and reference strains were compared using the M-fold web server (version 2.3)²⁷, with the loop fix set to untangled.

Results

Morphology and taxonomic identification

The unialgal culture was transferred to liquid BG-11 medium and identified as a nostocalean cyanobacterium, related to the Nostocales sensu lato group. Morphological characteristics, including colony morphology, cell size, and arrangement of cell types, were recorded (Fig. 1a–f), with heterocyst and akinetes measured. For comparison, the main similar genera microphotographs were shown in (Fig. 2).

Studied strain *Komarekiella* sp.1400, isolated from saline soil has a morphology very similar to other species of this genus. In nature, it adheres to the surface of saline soils, where it forms rusty- brown to dark brown mats. On the agar plates, it grew rapidly as a gelatinous biomass, forming various macroscopic colonies. (Fig. 1a). The colonies are aggregated loosely into macroscopic thalli on the surface and are covered in diffuent mucilage. They grow radially from the center to form a dense mat. The color of the thali is dark green, orange to dark brown. The trichomes were sometimes twisted, bent, or spiral-shaped, and hormogonia (8–15 cells) were dominant early in incubation (Fig. 1b). Cell color changed from pale green to dark brown as growth progressed.

Hormogonial cells were elongated, with two pre-heterocysts at each end (2.28 µm wide, 2.85 µm long). After 1–2 days, the terminal cells differentiated into heterocysts (Fig. 1c). Vegetative cells were rectangular, 5.7–5.9 µm wide, and 7.1–7.5 µm long, olive green in color, with thick, dark olive-green walls (Fig. 1d). Necrotic cells, which detached or fragmented, were also observed (Fig. 1e). Basal heterocysts were single, oblong, and ellipsoidal (12.5–13 µm long, 5.5–5.7 µm wide), while intercalary heterocysts were smaller and oblong (2.0–2.5 µm wide, 4.0–6.0 µm long) (Figs. 1f, 1g). Detached single heterocysts were seen (Fig. 1h), and akinetes appeared as chains at the ends or in the middle of filaments (Fig. 1i), typically oblong, 5.5–5.7 µm wide, and 11–11.5 µm long. A comparison of isolate 1400 with the type species *Komarekiella atlantica*²⁸, is shown in (Table 2). Morphological details of isolate 1400 are summarised in (Table 3).

Phylogenetic analyses

A 16S rDNA fragment was sequenced and compared to 396 cyanobacterial nucleotide sequences from GenBank for phylogenetic analysis. Query coverage and E-value of the hits were 99.98 to 100 and 1e⁻⁵⁰ respectively. The resulting maximum likelihood (ML) phylogenetic tree is shown in Fig. 3. While the main focus of this study is on the 16S rRNA gene sequence and its associated 16S–23S rRNA internal transcribed spacer (ITS) secondary structures, additional genes—*nifD*, *psbA*, and *rbcL*—were also analysed to further characterise isolate 1400 (Figs. 4–6). The phylogenetic tree includes a variety of genera and families, each forming distinct clusters. As shown in Fig. 3, each genus forms a distinct cluster or “cloud” with closely related genera. Notably, the genus *Komarekiella* is grouped with similar strains, including *Komarekiella atlantica* CCIBT 3483, CCIBT 3487, CCIBT 3486, CCIBT 3481, CCIBT 3552, *Komarekiella* sp. SJR-PJCV1, and *Komarekiella atlantica* strains HA4396-MV6, MTQ17-MM2, and MTQ8-MM1A.

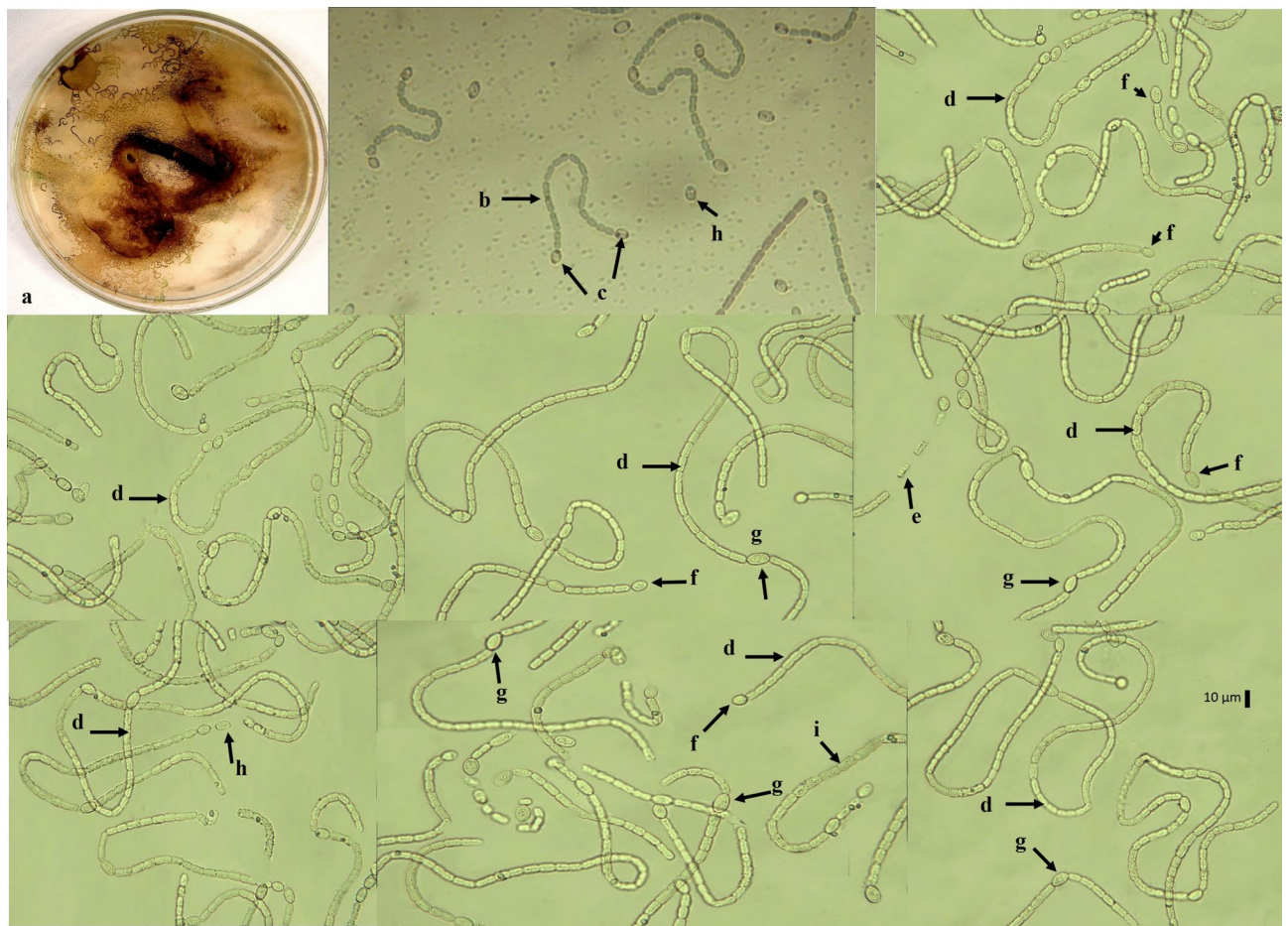


Fig. 1. Macroscopic growth with dark brown color of *Komarekiella* sp. isolate 1400 on solid media (a). Different light microphotographs (b–i) of *Komarekiella* sp. isolate 1400. Details are indicated with lowercase letters (b–i) according to the text.

Using phylogenetic trees, we compared the 16S rRNA and ITS p-distances of our strain with related *Komarekiella* strains, including CCIBT 3483, 3487, 3486, 3481, 3552, SJR-PJCV1, HA4396-MV6, MTQ17-MM2, and MTQ8-MM1A. *Komarekiella* sp. isolate 1400 grouped tightly with the type of strains of the *Komarekiella atlantica* (96.4% ultrafast bootstrap, Fig. 3). In the *nifD* phylogenetic analysis, isolate 1400 was positioned closed to *Nostoc* sp. PCC 7423 (AF442503, Fig. 4). However, in the *psbA* and *rbcL* analyses, it appeared on separate branches close to *Aliinostoc* (Figs. 5 and 6).

Phylogenetic trees were used to compare the ITS p-distances of our strain with related *Komarekiella* strains, including CCIBT 3487, 3552, MTQ17-MM2, MTQ8-MM1A, HA4396-MV6 clones C10B and C10A, CCIBT 3481, 3486, 3307, 3483, and *Komarekiella* sp. SJR-PJCV1. Results showed that *Komarekiella* sp. isolate 1400 shared high ITS sequence similarity with these strains, ranging from 98.20% with MTQ17-MM2 and MTQ8-MM1A to 98.47% with HA4396-MV6 clones C10B and C10A, CCIBT 3481, 3486, and 3483 (Table S4).

16S-23S rRNA ITS secondary structure

Ten reference sequences were used to search for ITS secondary structures. Ten different regions (D1–D1' helix, D2, D3, trRNA^{Ile} gene, V2, TrRNA^{Ala} gene, BOX B, BOX A, D4 and V3 helix) were found in the ITS secondary structure of the studied strains (Figs. 6–9). The D1–D1', V2 and Box-B regions of all the strains studied varied considerably in length and morphology (Figs. 7–10; Tables 4–6). The D1–D1' region included a terminal bilateral bulge (A), a bilateral bulge (B), a unilateral bulge (C), and a basal clamp (D) (Fig. 7). The D1–D1' helix length varied from 54 nt in *Komarekiella* HA4396-MV6 to 69 nt in *Komarekiella* isolate 1400, CCIBT 3552, and HA4396-MV6 (Tables 4–6).

Interestingly, the V2 region was found to be the same for all reference strains, except for *Komarekiella* sp. isolate 1400, which showed a different number of bilateral bulge (B) regions (Fig. 8) (Table 6).

Box-B was characterised by a terminal bilateral bulge (A), a bilateral bulge (B), and a basal clamp (C) (Fig. 9). Box-B lengths ranged from 84 nt in various *Komarekiella* strains (e.g., CCIBT 3483, CCIBT 3481, CCIBT 3487, CCIBT 3552, SJR-PJCV1, HA4396-MV6, MTQ17-MM2, and MTQ8-MM1A) to 86 nt in *Komarekiella* sp. isolate 1400 (Fig. 9). The V3 helix length and shape were identical between the studied strain and all reference strains (Fig. 10, Tables 6 and S5).

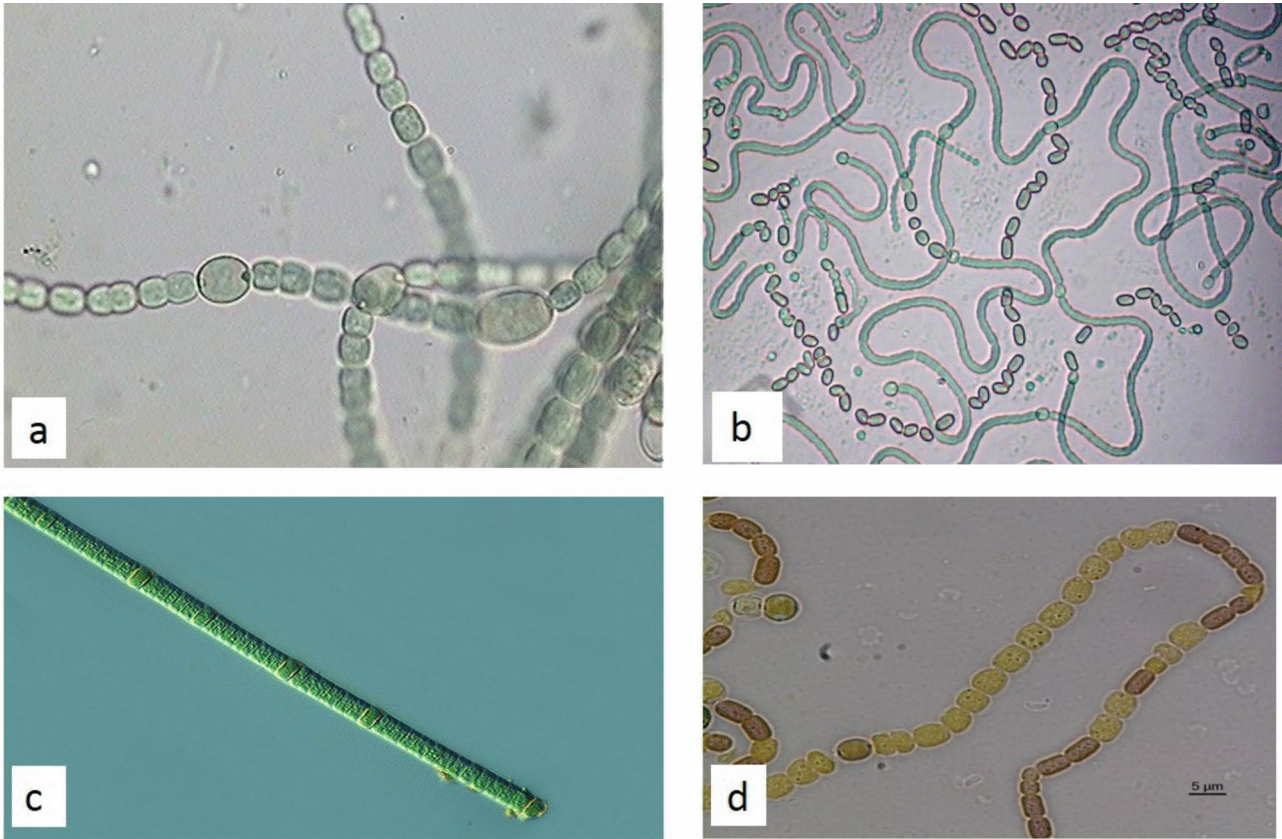


Fig. 2. Microphotographs of the close related species to genus *Komarekiella*: *Anabaena* sp. BN KY303913 (a), *Nostoc* sp. BN KY303912 (b), *Nodularia* sp. BN KY303914 (c), *Alinostoc* sp. (d), (400X).

	<i>Komarekiella atlantica</i>	<i>Komarekiella</i> sp. isolate 1400
Veg. cell length mean (range)	3–5	7.1–7.5
Veg. cell width mean (range)	3.4–5.5	5.7–5.9
Veg. cell length/width mean	0.89	1.25
Heterocyte length mean (range)	–	12.5–13
Heterocyte width mean (range)	3–5.5	5.5–5.7
Heterocyte length/width mean	–	2.27
Akinete length mean (range)	–	11–11.5
Akinete width mean (range)	3.5–6	5.5–5.7
Akinete length/width mean	–	2

Table 2. Comparison of morphological features between *Komarekiella* sp. isolate 1400 and *Komarekiella atlantica*.

Colonies size	Color	Color of thallus	Vegetative cells	Heterocytes	Hormogonia	Akinetes
0.5 to 9.0 mm	dark brown	light olive green to light brown	Completely oblong, 5.7–5.9 µm wide, 7.1–7.5 µm long	Completely oblong, 12.5–13 µm long, 5.5–5.7 µm wide	8–15 cells per hormogonium and presence of heterocysts at both ends	Oblong, 5.5–5.7 µm wide, 11–11.5 µm long

Table 3. Morphometric characteristics of *Komarekiella* sp. isolate 1400.

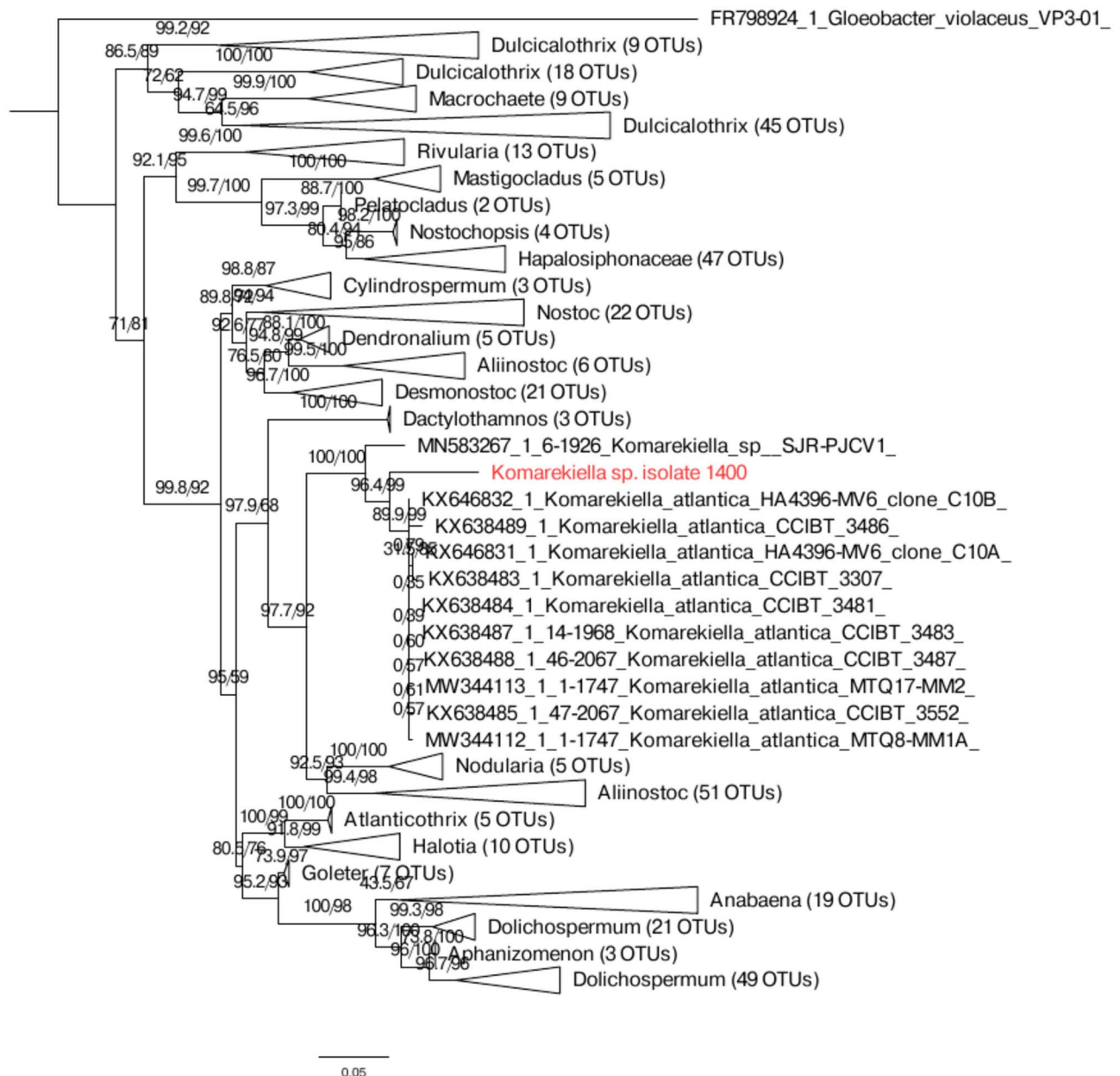


Fig. 3. Phylogenetic relationships among *Komarekiella* sp. isolate 1400 (in red) and related cyanobacteria based on 16S rDNA sequences (2028 bp) with *Gloeobacter violaceus* VP3-01 as outgroup. Numbers near nodes indicate standard bootstrap support (%) /ultrafast bootstrap support (%) for ML analyses. The scale bar indicates 0.05 substitutions per nucleotides.

These differences between the studied regions suggested, that our studied strain could be a potential new species for the genus *Komarekiella*, however they are usually not sensitive enough markers to distinguish a species from each other. The more in-deep studies of the strains including whole gene sequencing and more strain collections it seems to be needed.

Discussion

Recent substantial progress in the classification of the order Nostocales has led to the identification of several new taxa^{6,10,29–41}. In temperate climates, there has been a remarkable increase in the abundance and diversity of nostocacean taxa in recent decades. Specifically, the genus *Komarekiella*³. However, the genus has yet to be studied in many parts of Asia, and there are no records of this genus in Iran. Using a polyphasic approach, we study the molecular phylogenetic and morphometric evaluation of *Komarekiella* sp. from Iranian saline soils. A morphological comparison between *Komarekiella* sp. isolate 1400 and the reference strain *Komarekiella atlantica*³ revealed that the mean vegetative cell length/width, mean akinete cell length/width and mean heterocyst length/width of *Komarekiella* sp. isolate 1400 was greater than for known strains of *Komarekiella atlantica* (Table 2).

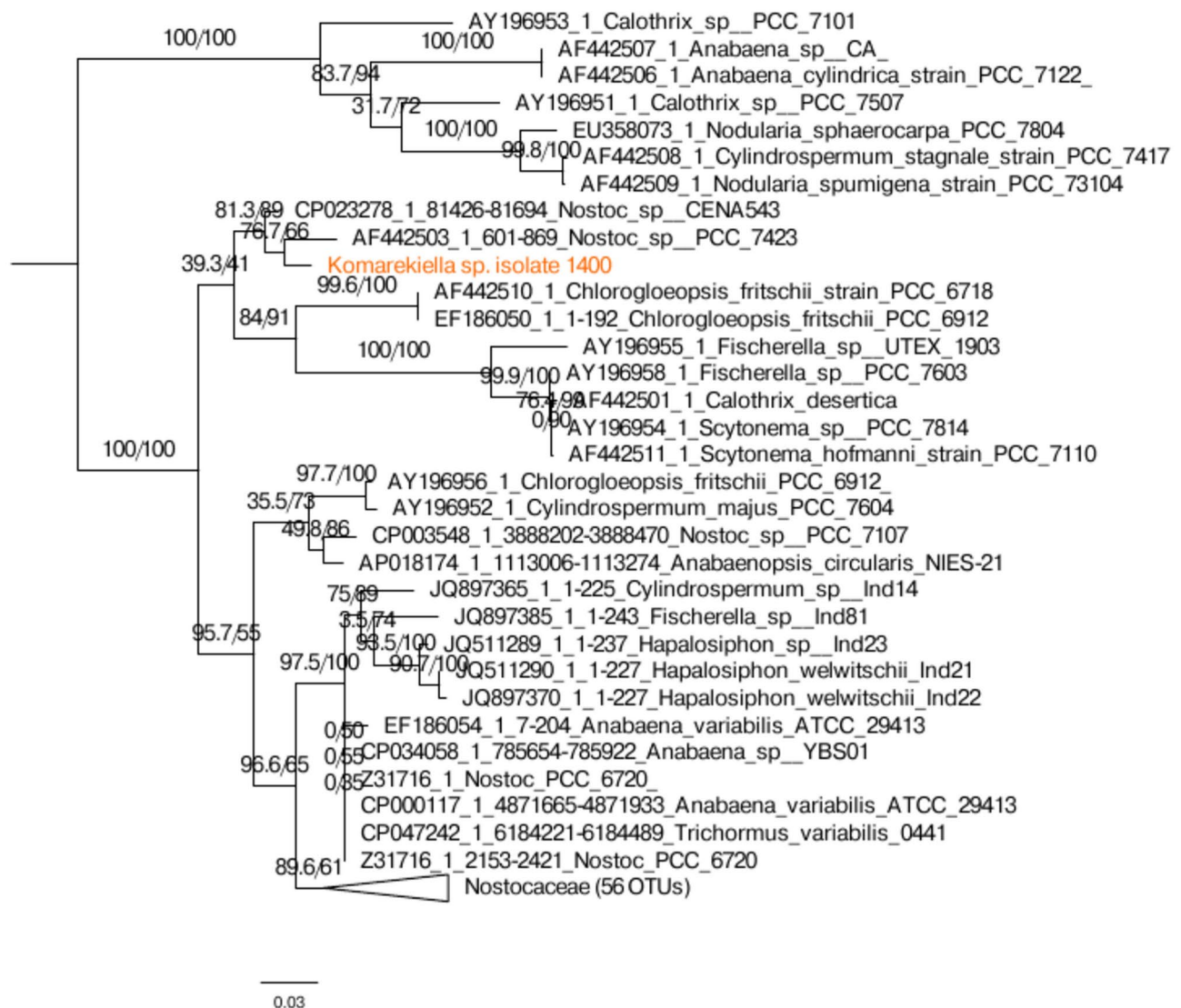


Fig. 4. Phylogenetic analyses displaying the relationship among the *nifD* gene sequences (247 bp). Numbers near nodes indicate standard bootstrap support (%) / ultrafast bootstrap support (%) for ML analyses. The scale indicates 0.03 mutations per amino acid position.

Morphological characteristics, along with 16S rRNA phylogenetic analysis and the analysis of secondary structures from the 16S-23S internal transcribed spacer (ITS), secondary structure analysis, effectively distinguished *Komarekiella* sp. isolate 1400 from other species within the genus. Phylogenetic analysis of the 16S rRNA gene sequence has shown that the taxa classified as *Nostoc* do not constitute a monophyletic group³. Therefore, new *Nostoc*-like genera that are phylogenetically closely related to *Nostoc sensu strictu* have been described: *Mojavia*⁴, *Desmonostoc*⁹, *Halotia*⁴², *Aliinostoc*⁶ and *Komarekiella* G.S³. In this study, the *Komarekiella* clade was clearly distinguished from other well-defined clades (*Hapalosiphonaceae*, *Nodularia*, *Aliinostoc*, and *Anabaena*), with *Komarekiella* sp. isolate 1400 firmly placed within its own clade based on the 16S rRNA phylogeny (Fig. 3).

The 16S-23S rRNA ITS and its secondary structure folding in *Komarekiella* sp. isolate 1400 differed from previously described species of *Komarekiella*. The dissimilarities in the D1-D1' and Box B helices (Figs. 7–10) suggest the novelty of isolate 1400 compared to related morphotypes, including strains such as CCIBT 3483, 3481, 3487, 3552, 3486, SJR-PJCV1, HA4396-MV6, MTQ17-MM2, and MTQ8-MM1A. However, due to some authors⁴³, these regions are not sensitive enough to separate taxa at the species level.

Additionally, our strain showed sequence alignment values with other similar taxa (Table S4)⁴⁴. According to⁴⁴, identities of <98.7% are considered as robust evidence for classifying the compared strains as different species⁴⁴. This is further supported by our results, with the calculated 16S rRNA p-distance between the studied strains and related species within the genus *Desmonostoc* ranging from 98.21 to 98.48%. These results broaden the understanding of the genetic variation and ecological range of the genus *Komarekiella* through a polyphasic analysis of *Komarekiella* sp. isolate 1400, demonstrating its presence in an atypical microhabitat within a saline

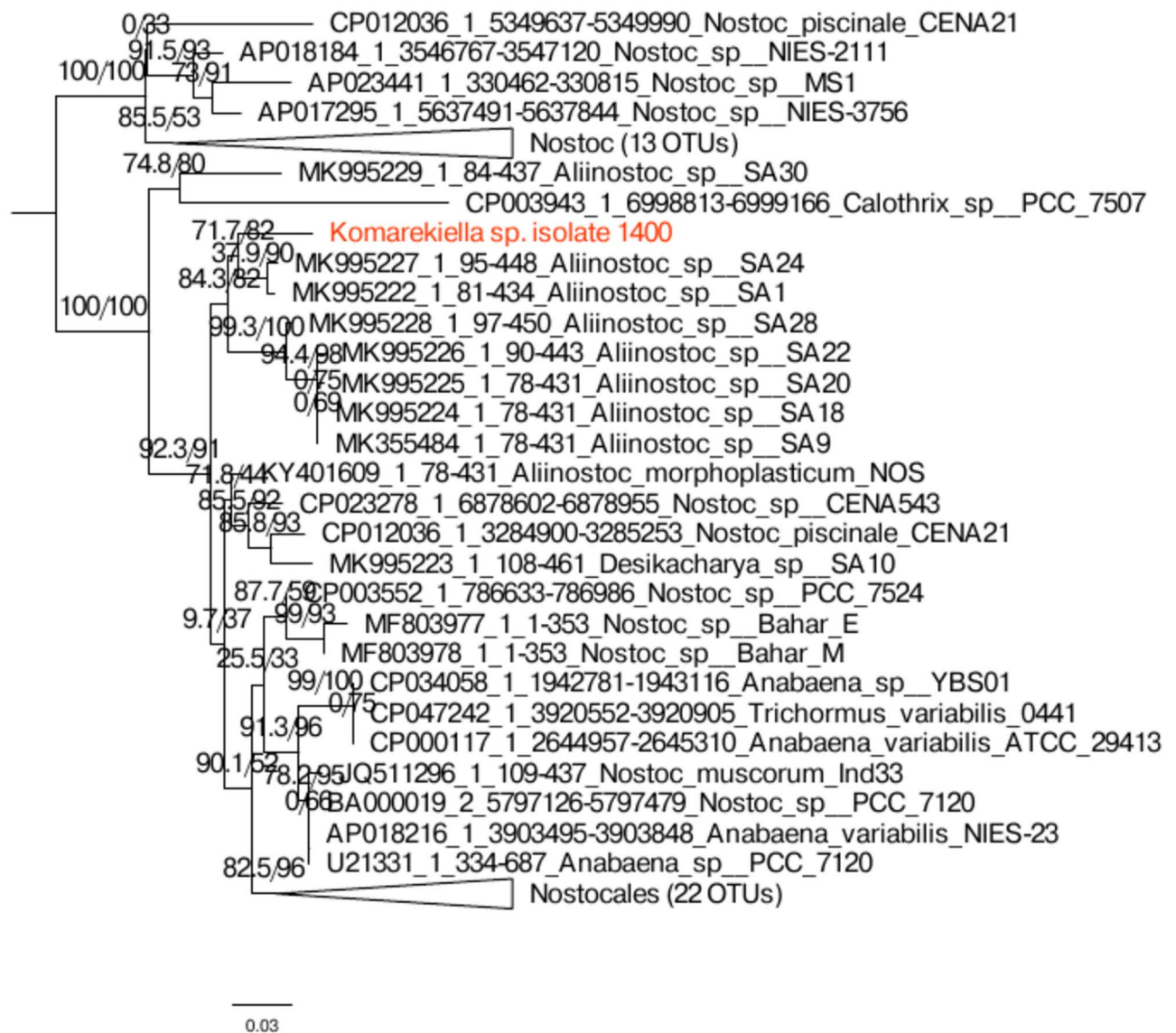


Fig. 5. Phylogenetic analyses displaying the relationship among the *psbA* gene sequences (445 bp). Numbers near nodes indicate standard bootstrap support (%) / ultrafast bootstrap support (%) for ML analyses. The scale indicates 0.03 mutations per amino acid position.

soil region. The identification of our strain will broaden the understanding of the geographical distribution of the genus *Komarekiella*, as well as adding the new habitats where it could be isolated.

The discovery of potentially halotolerant species of Nostocales cyanobacteria could also have a significant impact on the development and distribution of new types of biofertilisers. Heterocystous cyanobacteria with the ability to fix nitrogen represent the most promising alternatives to be used in agriculture to stabilise soils and modify their negative characteristics. Strains capable of producing mucilage, such as our *Komarekiella* strain, can stabilise damaged soils and slow down their erosion. They also produce polysaccharides that enrich the soil. Secondly, the use of native strains, which are already adapted to the harsh conditions of increased salinity and high osmotic stress, are better adapted to survive in this environment than the species that are transferred here from other types of habitat. For these potential future uses, the importance of characterising and isolating native strains from saline soils represents a significant contribution to future research with agricultural implications⁴⁵.

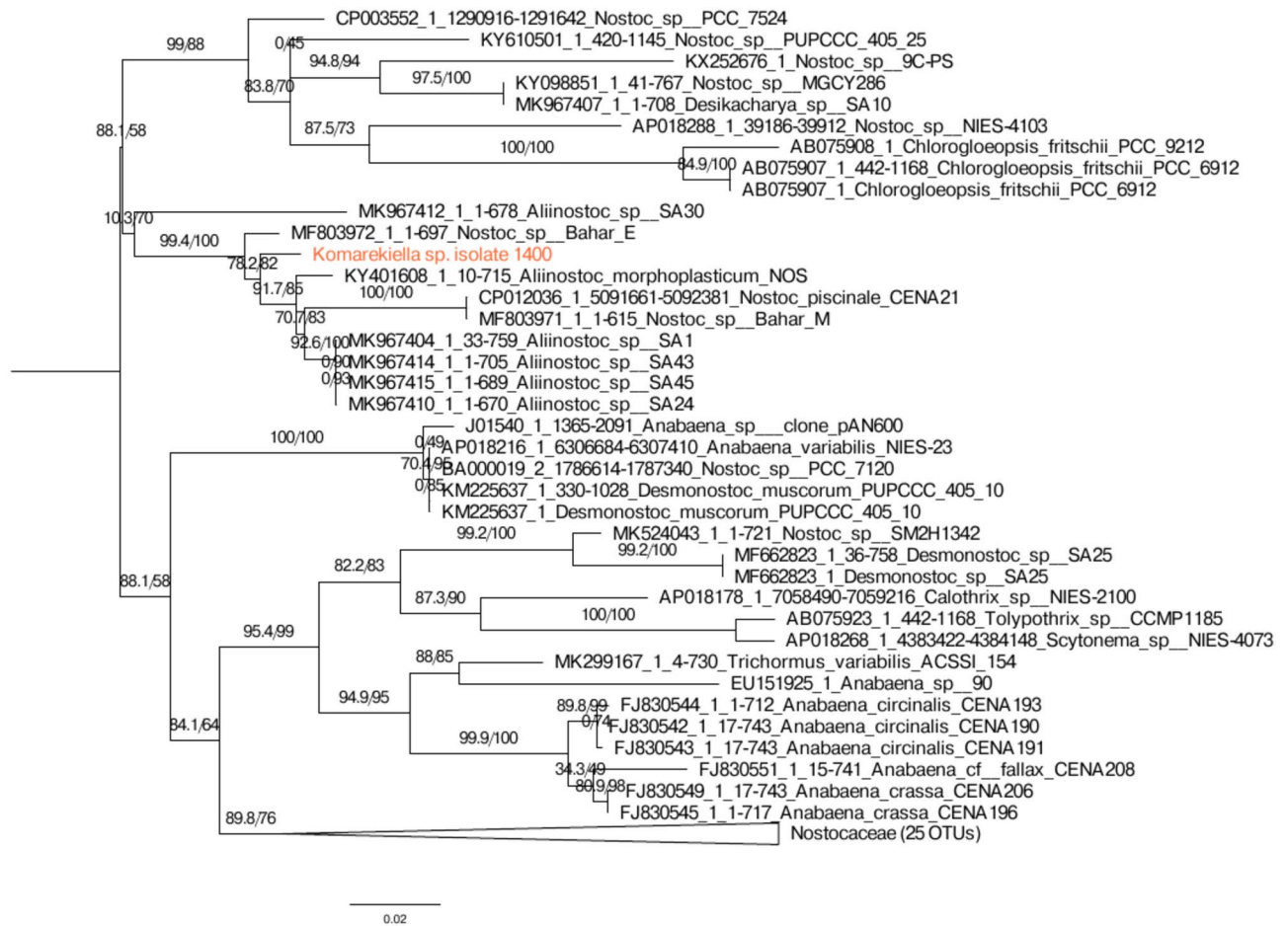


Fig. 6. Phylogenetic analyses displaying the relationship among the *rbcL* gene sequences (728 bp). Numbers near nodes indicate standard bootstrap support (%) /ultrafast bootstrap support (%) for ML analyses. The scale indicates 0.02 mutations per amino acid position.

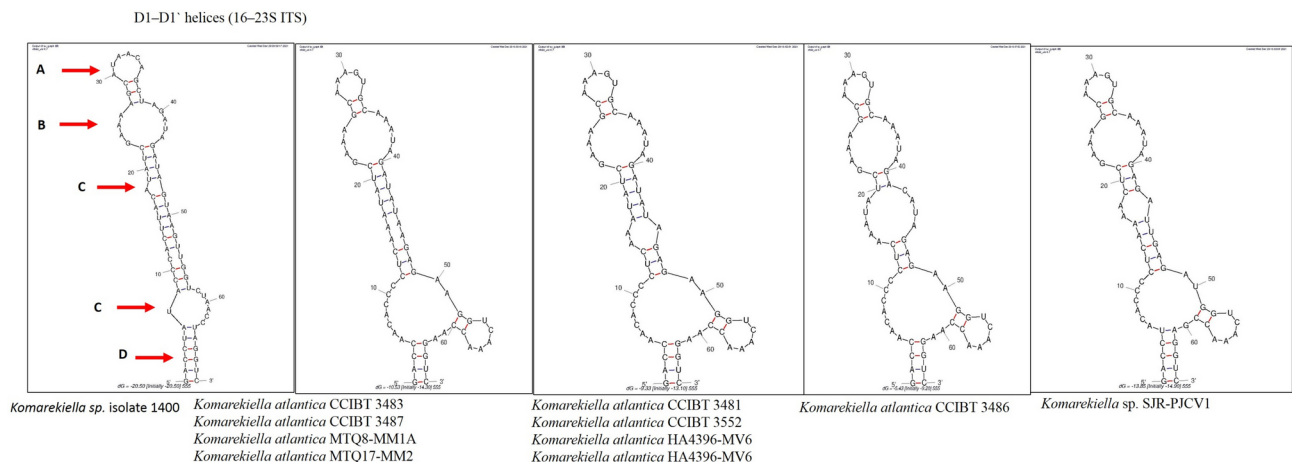


Fig. 7. Secondary structures of the D1–D1' helices from 16S–23S intergenic spacers. *Komarekiella* sp. isolate 1400, *Komarekiella atlantica* CCIBT 3483, *Komarekiella atlantica* CCIBT 3481, *Komarekiella atlantica* CCIBT 3487, *Komarekiella atlantica* CCIBT 3552, *Komarekiella atlantica* CCIBT 3486, *Komarekiella* sp. SJR-PJCV1, *Komarekiella atlantica* HA4396-MV6, *Komarekiella atlantica* HA4396-MV6, *Komarekiella atlantica* MTQ17-MM2 and *Komarekiella atlantica* MTQ8-MM1A.

V3	D 4 + spacer	BOX A	Spacer + BoxB + spacer	TrRNA ^{Ala} gene	spacer + V2 + spacer	trRNA ^{Ile} gene	D3 + spacer	D3	spacer + D2 + spacer	D1- D1, helix	Studied Strain and reference strains
54	20	11	86	73	82	74	12	4	39	69	<i>Komarekiella</i> sp. isolate 1400
54	20	11	84	73	82	74	12	4	39	66	KX638487.1:46-2067 <i>Komarekiella atlantica</i> CCIBT 3483
54	20	11	84	73	82	74	12	4	39	65	KX638484.1:47-2067 <i>Komarekiella atlantica</i> CCIBT 3481
54	20	11	84	73	82	74	12	4	39	66	KX638488.1:46-2067 <i>Komarekiella atlantica</i> CCIBT 3487
54	20	11	84	73	82	74	12	4	35	69	KX638485.1:47-2067 <i>Komarekiella atlantica</i> CCIBT 3552
54	20	11	84	73	82	74	12	4	39	65	KX638489.1:46-2066 <i>Komarekiella atlantica</i> CCIBT 3486
–	–	11	86	73	82	74	25	4	39	65	MN583267.1:6-1926 <i>Komarekiella</i> sp. SJR- PJCv1
54	20	11	84	73	82	74	12	4	50	54	KX646832.1:1-1746 <i>Komarekiella atlantica</i> HA4396-MV6
54	20	11	84	73	82	74	12	4	35	69	KX646831.1:1-1746 <i>Komarekiella atlantica</i> HA4396-MV6
54	20	11	84	73	82	74	12	4	39	66	MW344113.1:1-1747 <i>Komarekiella atlantica</i> MTQ17-MM2
54	20	11	84	73	82	74	12	4	39	66	MW344112.1:1-1747 <i>Komarekiella atlantica</i> MTQ8-MM1A

Table 4. Nucleotide lengths of the regions of the 16S–23S ITS of several studied strains.

Studied Strain and reference strains	D1-D1, helix				BOX B		
	Terminal bilateral bulge (A)	Bilateral bulge (B)	Unilateral bulge (C)	Basal clamp (D)	Terminal bilateral bulge (A)	Bilateral bulge (B)	Basal clamp (C)
	Number of nucleotides	Number of loops	Number of loops	Number of nucleotides	Number of nucleotides	Number of nucleotides	Number of nucleotides
<i>Komarekiella</i> sp. isolate 1400	8	1	2	12	6	10	10
KX638487.1:46-2067 <i>Komarekiella atlantica</i> CCIBT 3483	7	1	1	8	6	10	8
KX638484.1:47-2067 <i>Komarekiella atlantica</i> CCIBT 3481	7	3	0	8	6	10	8
KX638488.1:46-2067 <i>Komarekiella atlantica</i> CCIBT 3487	7	1	1	8	6	10	8
KX638485.1:47-2067 <i>Komarekiella atlantica</i> CCIBT 3552	7	3	0	8	6	10	8
KX638489.1:46-2066 <i>Komarekiella atlantica</i> CCIBT 3486	7	3	0	8	6	10	8
MN583267.1:6-1926 <i>Komarekiella</i> sp. SJR-PJCv1	7	3	0	10	6	10	8
KX646832.1:1-1746 <i>Komarekiella atlantica</i> HA4396-MV6	7	3	0	8	6	10	8
KX646831.1:1-1746 <i>Komarekiella atlantica</i> HA4396-MV6	7	3	0	8	6	10	8
MW344113.1:1-1747 <i>Komarekiella atlantica</i> MTQ17-MM2	7	1	1	8	6	10	8
MW344112.1:1-1747 <i>Komarekiella atlantica</i> MTQ8-MM1A	7	1	1	8	6	10	8

Table 5. Comparison of secondary structure of 16S-23S rRNA (D1-D1, helix and Box-B helix) between the *Komarekiella* sp. isolate 1400 with reference strains.

Studied Strain and reference strains	V2, helix			V3, helix		
	Terminal bilateral bulge (A)	Bilateral bulge (B)	Basal clamp (C)	Terminal bilateral bulge (A)	Bilateral bulge (B)	Basal clamp (C)
	Number of nucleotides	Number of loops	Number of nucleotides	Number of nucleotides	Number of loops	Number of nucleotides
Komarekiella sp. isolate 1400	8	3	8	6	1	10
KX638487.1:46-2067 Komarekiella atlantica CCIBT 3483	8	1	8	6	1	10
KX638484.1:47-2067 Komarekiella atlantica CCIBT 3481	8	1	8	6	1	10
KX638488.1:46-2067 Komarekiella atlantica CCIBT 3487	8	1	8	6	1	10
KX638485.1:47-2067 Komarekiella atlantica CCIBT 3552	8	1	8	6	1	10
KX638489.1:46-2066 Komarekiella atlantica CCIBT 3486	8	1	8	6	1	10
MN583267.1:6-1926 Komarekiella sp. SJR-PJCV1	8	1	8	6	1	10
KX646832.1:1-1746 Komarekiella atlantica HA4396-MV6	8	1	8	6	1	10
KX646831.1:1-1746 Komarekiella atlantica HA4396-MV6	8	1	8	6	1	10
MW344113.1:1-1747 Komarekiella atlantica MTQ17-MM2	8	1	8	6	1	10
MW344112.1:1-1747 Komarekiella atlantica MTQ8-MM1A	8	1	8	6	1	10

Table 6. Comparison of secondary structure of 16S-23S rRNA (V3, helix) between the *Komarekiella* sp. isolate 1400 with reference strains.

V2 helices (16–23S ITS) in

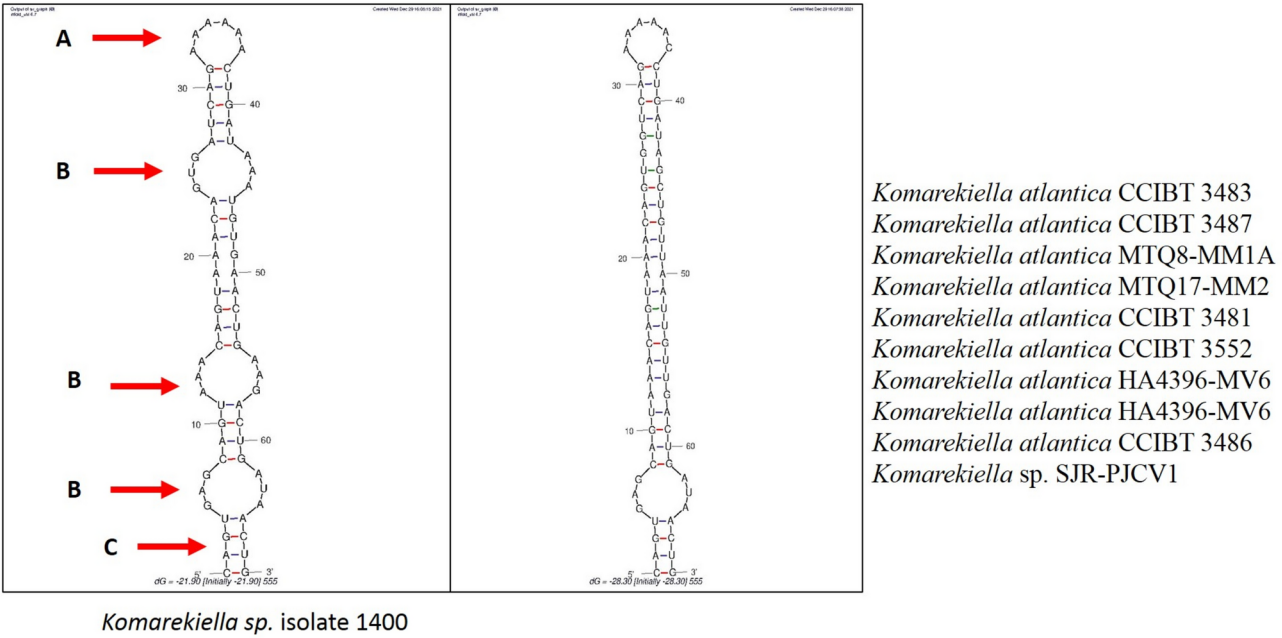


Fig. 8. Secondary structure comparisons of V2 from 16S–23S intergenic spacers. *Komarekiella* sp. isolate 1400, *Komarekiella atlantica* CCIBT 3483, *Komarekiella atlantica* CCIBT 3481, *Komarekiella atlantica* CCIBT 3487, *Komarekiella atlantica* CCIBT 3552, *Komarekiella atlantica* CCIBT 3486, *Komarekiella* sp. SJR-PJCV1, *Komarekiella atlantica* HA4396-MV6, *Komarekiella atlantica* HA4396-MV6, *Komarekiella atlantica* MTQ17-MM2 and *Komarekiella atlantica* MTQ8-MM1A.

Box B helices (16–23S ITS)

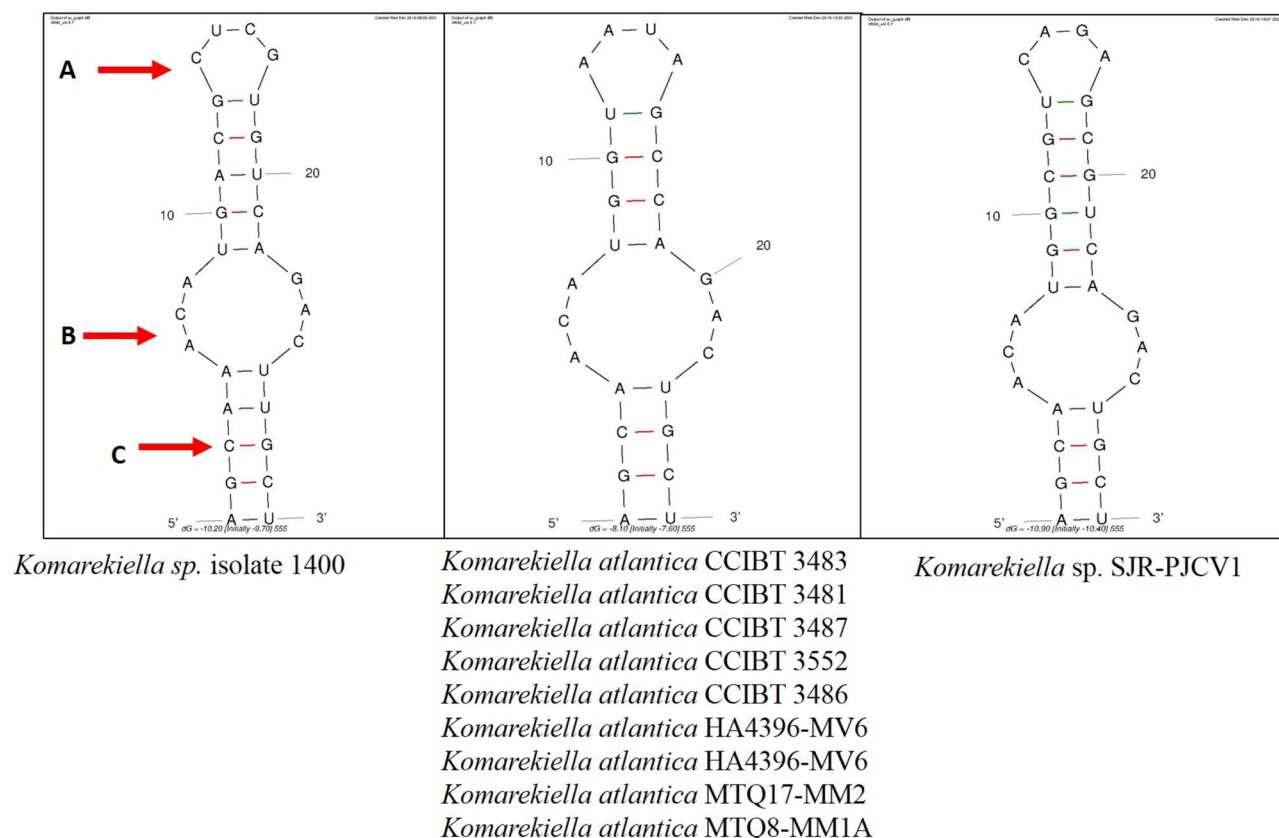


Fig. 9. Secondary structure comparisons of the Box B helices from 16S–23S intergenic spacers. *Komarekiella* sp. isolate 1400, *Komarekiella atlantica* CCIBT 3483, *Komarekiella atlantica* CCIBT 3481, *Komarekiella atlantica* CCIBT 3487, *Komarekiella atlantica* CCIBT 3552, *Komarekiella atlantica* CCIBT 3486, *Komarekiella* sp. SJR-PJCV1, *Komarekiella atlantica* HA4396-MV6, *Komarekiella atlantica* HA4396-MV6, *Komarekiella atlantica* MTQ17-MM2 and *Komarekiella atlantica* MTQ8-MM1A.

V3 helices (16–23S ITS)

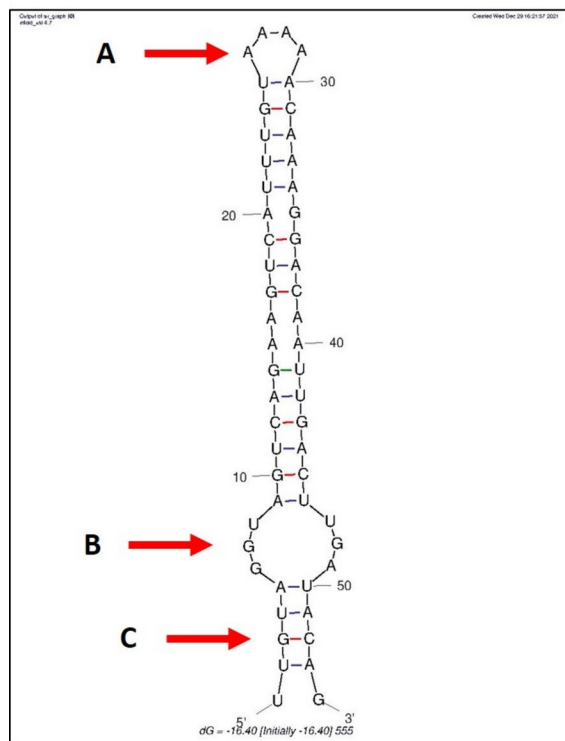
*Komarekiella* sp. isolate 1400*Komarekiella atlantica* CCIBT 3483 KX638488.1:*Komarekiella atlantica* CCIBT 3487 MW344112.1:*Komarekiella atlantica* MTQ8-MM1A MW344113.1:*Komarekiella atlantica* MTQ17-MM2*Komarekiella atlantica* CCIBT 3481 KX638485.1:*Komarekiella atlantica* CCIBT 3552 KX646832.1:*Komarekiella atlantica* HA4396-MV6 KX646831.1:*Komarekiella atlantica* HA4396-MV6*Komarekiella atlantica* CCIBT 3486*Komarekiella* sp. SJR-PJCV1

Fig. 10. Secondary structure comparisons of V3 from 16S–23S intergenic spacers. *Komarekiella* sp. isolate 1400, *Komarekiella atlantica* CCIBT 3483, *Komarekiella atlantica* CCIBT 3481, *Komarekiella atlantica* CCIBT 3487, *Komarekiella atlantica* CCIBT 3552, *Komarekiella atlantica* CCIBT 3486, *Komarekiella* sp. SJR-PJCV1, *Komarekiella atlantica* HA4396-MV6, *Komarekiella atlantica* HA4396-MV6, *Komarekiella atlantica* MTQ17-MM2 and *Komarekiella atlantica* MTQ8-MM1A.

Data availability

The datasets generated and/or analyzed during the current study are available for 16S rRNA in the [GenBank -] repository, [<https://www.ncbi.nlm.nih.gov/nucleotide/OP669676.1>] and accession number as: OP669676.1. RbcL are available in the [GenBank -] repository, [<https://www.ncbi.nlm.nih.gov/nucleotide/OP851553.1>] and accession number as: OP851553. *nifD* are available in the [GenBank -] repository, [<https://www.ncbi.nlm.nih.gov/nucleotide/OP851552.1>] and accession number as: OP851552. *psbA* are available in the [GenBank -] repository, [<https://www.ncbi.nlm.nih.gov/nucleotide/OP846527.1>] and accession number as: OP846527. Other sequences used in the study are also available in the GenBank repository, [<https://www.ncbi.nlm.nih.gov>] under the accessory numbers mention in the phylogenetic trees. For other raw data contact the corresponding authors.

Received: 15 November 2024; Accepted: 5 March 2025

Published online: 14 March 2025

References

- Múnera-Porras, L. M., García-Londoño, S. & Ríos-Osorio, L. A. Action mechanisms of plant growth promoting cyanobacteria in crops in situ: a systematic review of literature. *Int. J. Agron.* **2020**, 1–9 (2020).
- Nowruzi, B. & Hutarova, L. Structural and functional genes, and highly repetitive sequences commonly used in the phylogeny and species concept of the phylum cyanobacteria. *Cryptogamie, Algologie* **44** (3), 59–84 (2023).
- Hentschke, G. S. et al. Phylogenetic placement of *Dapisostemon* gen. nov. and *Streptostemon*, two tropical heterocytous genera (Cyanobacteria). *Phytotaxa* **245** (2), 129–143 (2016).
- Řeháková, K. et al. Morphological and molecular characterization of selected desert soil cyanobacteria: three species new to science including *Mojavia pulchra* gen. et. sp. nov.. *Phycologia* **46** (5), 481–502 (2007).
- Genuario, D. B. et al. Heterocyte-forming cyanobacteria from Brazilian saline-alkaline lakes. *Mol. Phylogenet. Evol.* **109**, 105–112 (2017).
- Bagchi, S. N., Dubey, N. & Singh, P. Phylogenetically distant clade of Nostoc-like taxa with the description of *Aliinostoc* gen. nov. and *Aliinostoc morphoplasticum* sp. nov.. *Int. J. Syst. Evol. Microbiol.* **67** (9), 3329–3338 (2017).
- Saraf, A. G., Dawda, H. G. & Singh, P. *Desikacharya* gen. nov., a phylogenetically distinct genus of Cyanobacteria along with the description of two new species, *Desikacharya nostocoides* sp. nov. and *Desikacharya soli* sp. nov., and reclassification of Nostoc thermotolerans to *Desikacharya thermotolerans* comb. nov.. *Int. J. System. Evol. Microbiol.* **69** (2), 307–315 (2019).
- Cai, F. et al. *Desmonostoc danxiaense* sp. nov. (Nostocales, Cyanobacteria) from Danxia mountain in China based on polyphasic approach. *Phytotaxa* **367** (3), 233–244 (2018).

9. Hrouzek, P. et al. Description of the cyanobacterial genus *Desmonostoc* gen. nov. including *D. muscorum* comb. nov. as a distinct phylogenetically coherent taxon related to the genus *Nostoc*. *Fottea* **13** (2), 201–213 (2013).
10. de Alvarenga, L. V. et al. Extending the ecological distribution of *Desmonostoc* genus: proposal of *Desmonostoc salinum* sp. nov., a novel Cyanobacteria from a saline–alkaline lake. *Int. J. Syst. Evolution. Microbiol.* **68** (9), 2770–2782 (2018).
11. Jung, P. et al. Opening the gap: Rare lichens with rare cyanobionts—Unexpected cyanobiont diversity in cyanobacterial lichens of the order Lichinales. *Front. Microbiol.* **12**, 728378 (2021).
12. Panou, M. & Gkelis, S. Unravelling unknown cyanobacteria diversity linked with HCN production. *Mol. Phylogenet. Evol.* **166**, 107322 (2022).
13. Brown, A. O. et al. A new species of cryptic cyanobacteria isolated from the epidermis of a bottlenose dolphin and as a bioaerosol. *Phycologia* **60** (6), 603–618 (2021).
14. Nowruzi, B. & Soares, F. *Alborzia kermanshahica* gen. nov., sp. nov. (Chroococcales, Cyanobacteria), isolated from paddy fields in Iran. *Int. J. Syst. Evolution. Microbiol.* **71** (6), 004828 (2021).
15. Nowruzi, B. & Shalygin, S. Multiple phylogenies reveal a true taxonomic position of *Dulcicalothrix alborzica* sp. nov. (Nostocales, Cyanobacteria). *Fottea* **21** (2), 235–246 (2021).
16. Nowruzi, B., Fahimi, H. & Ordodari, N. Molecular phylogenetic and morphometric evaluation of *Calothrix* sp. N42 and *Scytonema* sp. N11. *Rostaniha* **18** (2), 210–221 (2017).
17. Nowruzi, B. et al. A new strain of *Neowestiellopsis* (Hapalosiphonaceae): first observation of toxic soil cyanobacteria from agricultural fields in Iran. *BMC Microbiol.* **22** (1), 107 (2022).
18. Nowruzi, B. et al. Characterization of *Neowestiellopsis persica* A1387 (Hapalosiphonaceae) based on the *cpc A*, *psb A*, *rpo C1*, *nif H* and *nif D* gene sequences. *BMC Ecol. Evol.* **24** (1), 57 (2024).
19. Nowruzi, B. Phylogenetic study of *Aliinostoc* species (Cyanobacteria) using *pc-igs*, *nifH* and *mcy* as markers for investigation of horizontal gene transfer. *Acta Biol. Slovenica* **65** (2), 104–115 (2022).
20. Singh, P. et al. A new species of *Scytonema* isolated from Bilaspur, Chhattisgarh India. *J. System. Evol.* **54** (5), 519–527 (2016).
21. Rippka, R. et al. Generic assignments, strain histories and properties of pure cultures of cyanobacteria. *Microbiology* **111** (1), 1–61 (1979).
22. Komárek, J. et al. Taxonomic classification of cyanoprokaryotes (cyanobacterial genera) 2014, using a polyphasic approach. *Preslia* **86** (4), 295–335 (2014).
23. Hall, T. A. BioEdit: a user-friendly biological sequence alignment editor and analysis program for Windows 95/98/NT. *Nucleic Acids Symp. Ser.* **41**, 95–98 (1999).
24. Nguyen, L. T. et al. IQ-TREE: a fast and effective stochastic algorithm for estimating maximum-likelihood phylogenies. *Mol. Biol. Evol.* **32** (1), 268–274 (2015).
25. Ronquist, F. et al. MrBayes 3.2: efficient Bayesian phylogenetic inference and model choice across a large model space. *System. Biol.* **61** (3), 539–542 (2012).
26. Johansen, J. R. et al. Utility of 16S–23S ITS sequence and secondary structure for recognition of intrageneric and intergeneric limits within cyanobacterial taxa: *Leptolyngbya corticola* sp. nov. (Pseudanabaenaceae, Cyanobacteria). *Nova Hedwigia* **92** (3), 283 (2011).
27. Zuker, M. Mfold web server for nucleic acid folding and hybridization prediction. *Nucleic Acids Res.* **31** (13), 3406–3415 (2003).
28. Hentschke, G. S. et al. *Komarekiella atlantica* gen. et sp. nov. (Nostocaceae, Cyanobacteria): a new subaerial taxon from the Atlantic Rainforest and Kauai Hawaii. *Fottea* **17** (2), 178–190 (2017).
29. Alvarenga, D. O. et al. *Kryptousia macronema* gen. nov., sp. nov. and *Kryptousia microlepis* sp. nov., nostoclean cyanobacteria isolated from phyllospheres. *Int. J. Syst. Evol. Microbiol.* **67** (9), 3301–3309 (2017).
30. Galhano, V. et al. Morphological, biochemical and molecular characterization of *Anabaena*, *Aphanizomenon* and *Nostoc* strains (Cyanobacteria, Nostocales) isolated from Portuguese freshwater habitats. *Hydrobiologia* **663**, 187–203 (2011).
31. Nowruzi, B. & Lorenzi, A. S. Morphological and molecular characterization of *Goleter* sp. (Nostocales, Nostocaceae) isolated from freshwater in Iran. *Cryptogamie, Algologie* **45** (4), 39–51 (2024).
32. Nowruzi, B. & Porzani, S. J. The phylogenetic reconstruction of biosynthesizing genes from Cyanobacteria isolated from Ziarat waterfall of Golestan province. *Iran. J. Botany* **29** (2), 187–200 (2023).
33. Nowruzi, B. & Lorenzi, A. S. Molecular phylogeny of two *Aliinostoc* isolates from a paddy field. *Plant Syst. Evol.* **309** (2), 11 (2023).
34. Nowruzi, B. & Afshari, G. In silico analysis of molecular phylogeny of genes involved in the synthesis of bioactive compounds in cyanobacteria strains located in Tehran Cascade. *Jentashapir J. Cell. Mol. Biol.* <https://doi.org/10.5812/jcmb-132400> (2023).
35. Nowruzi, B., Becerra-Absalón, I. & Metcalf, J. S. A novel microcystin-producing cyanobacterial species from the genus *desmonostoc*, *desmonostoc alborizicum* sp. nov., isolated from a water supply system of Iran. *Curr. Microbiol.* **80** (1), 49 (2023).
36. Rivandi, M., Nowruzi, B. & Fahimi, H. Molecular phylogenetic study of toxic cyanobacterium *Anabaena* sp. strain B3 isolated from Lavasan Lake, Tehran (Iran). *Rostaniha* **22** (1), 120–133 (2021).
37. Nowruzi, B. & Lorenzi, A. S. Production of the neurotoxin homoanatoxin-a and detection of a biosynthetic gene cluster sequence (*anaC*) from an Iranian isolate of *Anabaena*. *South Afr. J. Botany* **139**, 300–305 (2021).
38. Zapomělová, E. et al. Polyphasic characterization of eight planktonic *Anabaena* strains (Cyanobacteria) with reference to the variability of 61 *Anabaena* populations observed in the field. *Hydrobiologia* **639**, 99–113 (2010).
39. Krienitz, L., Dadheech, P. K. & Kotut, K. Mass developments of the cyanobacteria *Anabaenopsis* and *Cyanospira* (Nostocales) in the soda lakes of Kenya: ecological and systematic implications. *Hydrobiologia* **703**, 79–93 (2013).
40. Mishra, S. et al. Weighted morphology: a new approach towards phylogenetic assessment of Nostocales (Cyanobacteria). *Protoplasma* **252**, 145–163 (2015).
41. González-Resendiz, L. et al. Two new species of *Phyllonema* (Rivulariaceae, Cyanobacteria) with an emendation of the genus. *J. Phycol.* **54** (5), 638–652 (2018).
42. Genuario, D. B. et al. *Halotia* gen. nov., a phylogenetically and physiologically coherent cyanobacterial genus isolated from marine coastal environments. *Int. J. Syst. Evol. Microbiol.* **65** (Pt_2), 663–675 (2015).
43. Dvořák, P. et al. Population genomics meets the taxonomy of cyanobacteria. *Algal Res.* **72**, 103128 (2023).
44. Yarza, P. et al. Uniting the classification of cultured and uncultured bacteria and archaea using 16S rRNA gene sequences. *Nat. Rev. Microbiol.* **12** (9), 635–645 (2014).
45. Devi, S., Rani, N. & Sagar, A. Bioreclamatory studies on salt affected soil by using cyanobacterial biofertilizers. *Plant Arch.* <https://doi.org/10.51470/PLANTARCHIVES.2021.v21.no2.065> (2021).

Author contributions

Conceptualization, B.N.; methodology, M.Gh.; software, B.N.; validation, B.N.; formal analysis, B.N, R. N, L.H investigation, B.N.; resources, B.N and S.H.

Declarations

Competing interests

The authors declare no competing interests.

Additional information

Supplementary Information The online version contains supplementary material available at <https://doi.org/10.1038/s41598-025-93257-1>.

Correspondence and requests for materials should be addressed to S.H. or B.N.

Reprints and permissions information is available at www.nature.com/reprints.

Publisher's note Springer Nature remains neutral with regard to jurisdictional claims in published maps and institutional affiliations.

Open Access This article is licensed under a Creative Commons Attribution-NonCommercial-NoDerivatives 4.0 International License, which permits any non-commercial use, sharing, distribution and reproduction in any medium or format, as long as you give appropriate credit to the original author(s) and the source, provide a link to the Creative Commons licence, and indicate if you modified the licensed material. You do not have permission under this licence to share adapted material derived from this article or parts of it. The images or other third party material in this article are included in the article's Creative Commons licence, unless indicated otherwise in a credit line to the material. If material is not included in the article's Creative Commons licence and your intended use is not permitted by statutory regulation or exceeds the permitted use, you will need to obtain permission directly from the copyright holder. To view a copy of this licence, visit <http://creativecommons.org/licenses/by-nc-nd/4.0/>.

© The Author(s) 2025, corrected publication 2025